

### Three kinds of intermittency in a nonlinear mechanical system

S. Chatterjee and A. K. Mallik\*

Department of Mechanical Engineering, Indian Institute of Technology, Kanpur Uttar Pradesh 208016, India

(Received 21 August 1995)

All three different types of classical, Pomeau-Manneville intermittencies along with a fourth kind following a subcritical pitchfork bifurcation have been identified in a single mathematical model. The mathematical model corresponds to a van der Pol oscillator with an impact damper.

PACS number(s): 05.45.+b, 62.30.+d

#### I. INTRODUCTION

Nonlinear systems are capable of exhibiting different kinds of instabilities and catastrophes which lead to complicated dynamic evolutions. Intermittency catastrophes occupy an important place in the whole spectrum of these dynamic complexities. A temporal intermittency signature is characterized by phases of regular oscillation (so called laminar phases) interrupted by chaotic bursts. A comprehensive theoretical model of intermittency was put forward by Pomeau and Manneville (PM model) [1-3]. Three catastrophic (subcritical) local bifurcations viz., saddle-node, Hopf, and subharmonic bifurcations are known to generate three types of PM intermittencies viz., type I, II, and III, respectively. Observations of different kinds of intermittencies in experimental and theoretical models [4-7] have supported the above mentioned theory. It is now known that many hydrodynamic instabilities (as well as solid-mechanical and electrical instabilities) are related to these intermittencies. But no single model is known to demonstrate all the three kinds of PM intermittencies. It would be interesting to observe these intermittencies in a single model. The purpose of this paper is to discuss such a model consisting of a van der Pol type mechanical oscillator with an impact damper. Apart from the three types of PM intermittencies, another new kind of intermittency caused by a subcritical symmetry-breaking bifurcation is also observed in this model.

#### II. EQUATIONS OF MOTION

An impact damper in the form of a loose secondary mass is often used to control the vibrations of a mechanical oscillator which may be linear, nonlinear or self-excited [8]. In this paper, the primary vibrating system is modeled as a mechanical oscillator consisting of a mass ( $m_1$ ), a linear spring (of stiffness  $K_1$ ) and a damper exerting a nonlinear, van der Pol type damping force. This system is shown in Fig. 1(a) where the prime denotes differentiation with respect to time  $t$ . The mass  $m_1$  is excited by a harmonic force  $F \cos \omega t$ . The loose secondary mass  $m_2$  goes into repeated collisions with both ends of the container (fixed to  $m_1$ ) of length  $d$ . In this process the response of  $m_1$  is controlled by transfer of momentum and dissipation of energy. The differential equations describing the motion of the system between two consecu-

tive collisions can be written in the following nondimensional form:

$$\ddot{Z}_1 + \varepsilon \dot{Z}_1 (Z_1^2 - 1) + Z_1 = F_0 \cos(\Omega \tau) \tag{1a}$$

and

$$\ddot{Z}_p = 0 \quad \forall |Z_1 - Z_p| < d_0 \tag{1b}$$

with  $\omega_0 = (K_1/m_1)^{1/2}$ ,  $x_0 = \sqrt{g_1}$ ,  $\Omega = \omega/\omega_0$ ,  $F_0 = F/(m_1 x_0 \omega_0^2)$ ,  $\varepsilon = e_1 x_0^2 / (m_1 \omega_0)$ ,  $Z_1 = x_1/x_0$ ,  $Z_p = x_2/x_0$ ,  $d_0 = d/2x_0$ ,  $\tau = \omega_0 t$  and the dot denotes differentiation with respect to  $\tau$ . It may be noted that  $m_2$  is assumed to be a free particle, except at the instants of collisions.

When  $|Z_1 - Z_p| = d_0$ , a collision occurs satisfying the following conditions:

$$\dot{Z}_1^- = \alpha_1 \dot{Z}_p^- + \alpha_2 \dot{Z}_p^+,$$

$$\dot{Z}_1^+ = \alpha_3 \dot{Z}_p^- + \alpha_4 \dot{Z}_p^+,$$

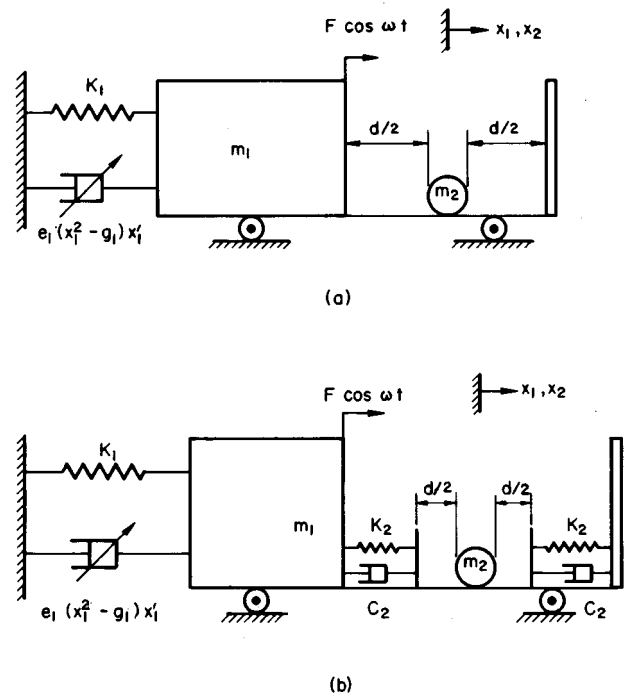


FIG. 1. van der Pol oscillator with an impact damper. (a) Zero contact time, (b) finite contact time.

\*Electronic address: akmallik@iitk.ernet.in

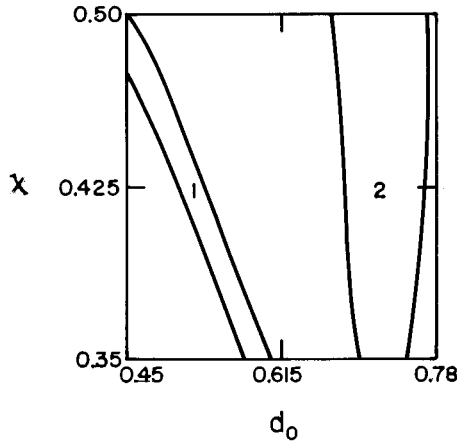


FIG. 2. Windows of periodic solutions in  $\chi-d_0$  plane.  $r_m=0.1$ ,  $\epsilon=0.1$ . Regions of periodic solutions are labeled by 1 and 2.

where the superscripts + and - denote, respectively, the conditions after and before impacts. Using the conservation of total linear momentum and the definition of the coefficient of restitution it is easy to obtain  $\alpha_i$ 's as follows:

$$\alpha_1 = (\chi - r_m)/(1 + \chi),$$

$$\alpha_2 = (1 + r_m)/(1 + \chi),$$

$$\alpha_3 = \chi(1 + r_m)/(1 + \chi),$$

$$\alpha_4 = (1 - r_m\chi)/(1 + \chi),$$

where  $\chi$  is the coefficient of restitution and  $r_m = m_2/m_1$ , is the mass ratio.

An alternative way of modeling an impact damper would be through the introduction of a spring and a linear viscous damper as shown in Fig. 1(b). In this model, the time interval of contact (between  $m_2$  and the container sidewalls) during collision is nonzero. The differential equations describing the motion of such a system are written in the following nondimensional form:

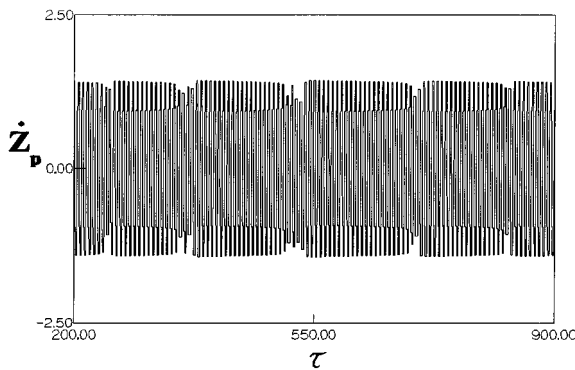


FIG. 3. Signature of type I intermittency.  $\epsilon=0.1$ ,  $r_m=0.1$ ,  $\chi=0.35$ ,  $d_0=0.77$

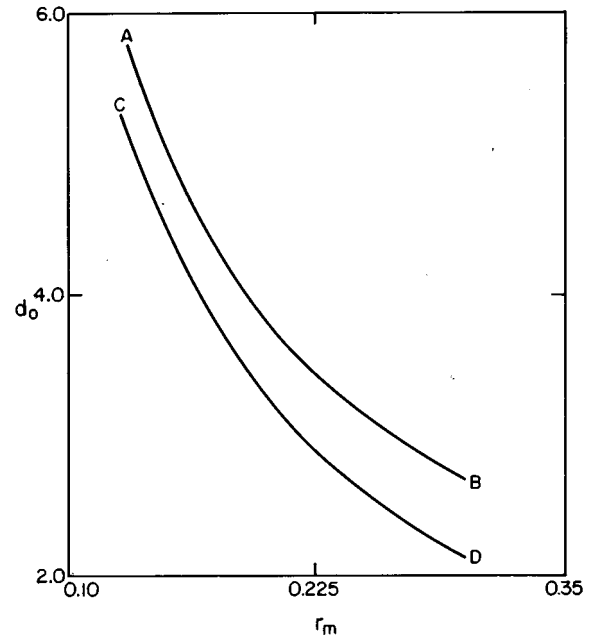


FIG. 4. Bifurcation set in  $r_m-d_0$  plane.  $\Omega=1$ ,  $\chi=0.7$ ,  $F_0=0.5$ ,  $\epsilon=0.1$ . The zone enclosed between the lines AB and CD corresponds to stable symmetric motion with two impacts per cycle. AB and CD correspond to supercritical and subcritical Hopf bifurcations, respectively.

$$\ddot{Z}_1 + \epsilon(Z_1^2 - 1)\dot{Z}_1 + Z_1 + r_1\Phi_1(Z_2) + 2\xi_c\sqrt{r_1r_m}\Phi_2(Z_2)\dot{Z}_2 = F_0\cos\Omega\tau \tag{2a}$$

and

$$\ddot{Z}_2 + r_1\Phi_1(Z_2)/r_m + 2\xi_c\sqrt{r_1/r_m}\Phi_2(Z_2)\dot{Z}_2 = \ddot{Z}_1, \tag{2b}$$

where

$$\Phi_1(Z_2) = (Z_2 - d_0)U(Z_2 - d_0) + (Z_2 + d_0)U(-Z_2 - d_0),$$

$$\Phi_2(Z_2) = U(Z_2 - d_0) + U(-Z_2 - d_0),$$

when  $U(\cdot)$  is Heaviside's step function defined as

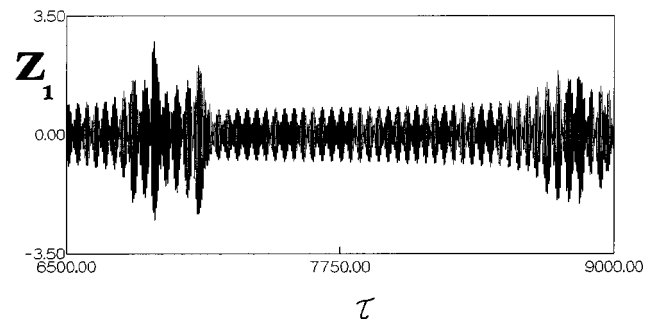


FIG. 5. Signature of type II intermittency.  $\Omega=1$ ,  $\chi=0.7$ ,  $F_0=0.5$ ,  $r_m=0.25$ ,  $d_0=2.49$ .

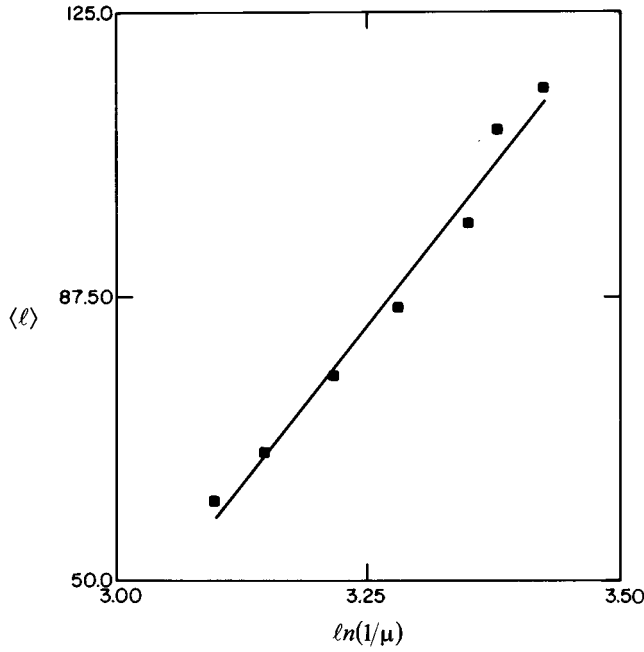


FIG. 6. Scaling law of type II intermittency. The parameter values are given in Fig. 5.

$$U(\zeta) = 1 \quad \forall \zeta > 0$$

$$= 0 \quad \forall \zeta < 0$$

and  $r_1 = K_2/K_1$ ,  $Z_2 = (x_1 - x_2)/x_0$  and the damping ratio  $\xi_c$  is obtained in terms of the coefficient of restitution  $\chi$  (used in the first model) as [9]

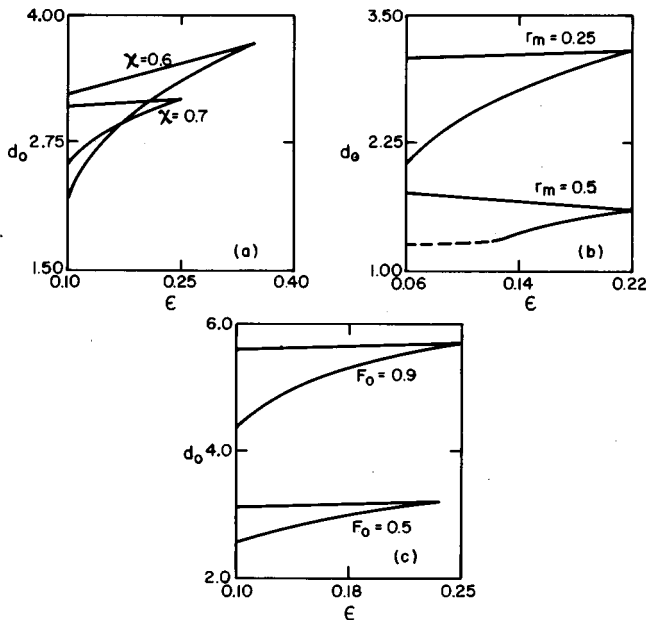


FIG. 7. Bifurcation sets in  $\epsilon-d_0$  plane.  $\Omega=1$ . (a)  $F_0=0.5$ ,  $r_m=0.25$ ; (b)  $F_0=0.5$ ,  $\chi=0.7$ ; (c)  $\chi=0.7$ ,  $r_m=0.25$ . —Hopf bifurcation (the upper line corresponds to supercritical bifurcation and the lower line corresponds to subcritical bifurcation), - - - pitchfork bifurcation (subcritical).

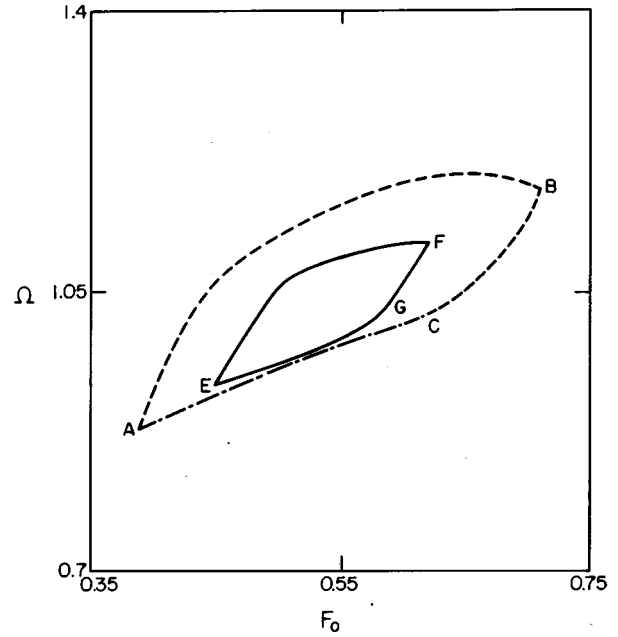


FIG. 8. Bifurcation set in  $F_0-\Omega$  plane.  $\chi=0.7$ ,  $\epsilon=0.1$ .  $AB$ —supercritical Hopf bifurcation,  $BC$ —subcritical Hopf bifurcation,  $CA$ —subcritical pitchfork bifurcation:  $d_0=1.6$ ,  $r_m=0.45$ .  $EF$ —supercritical Hopf bifurcation,  $EGF$ —subcritical Hopf bifurcation:  $d_0=2.9$ ,  $r_m=0.25$ .

$$\xi_c = C_2/2\sqrt{K_2 m_2} = - \frac{\ln(\chi)}{((1+r_m)\{\pi^2 + [\ln(\chi)]^2\})^{1/2}} \cdot (3)$$

This expression is valid except in a small neighborhood of  $\chi=0$ .

With a very high numerical value of  $r_1$  [ $\sim o(10^5)$ ] in Eqs. (2), the results obtained from both models described above are found to be quite close. However, it has been seen that the second model described by Eqs. (2) offers special advantages over Eqs. (1) during numerical integration.

### III. RESULTS AND DISCUSSIONS

An analytical method based on the equivalent piecewise linearization (EPL) technique [10] is used to construct the periodic solutions of Eqs. (1) and the method of error propagation [10] is used to analyze the stability of these solutions. A fourth order Runge-Kutta-Merson algorithm with adaptive step size control is used for numerical integration of Eqs. (2). This revealed different types of intermittency routes to chaos which are discussed below.

#### A. Type I intermittency

First consider the autonomous vibration, i.e.,  $F_0=0$ . It should be noted that due to the self-excitation provided by the van der Pol type damping force, this autonomous vibration can be sustained (in the form of a so-called limit cycle). The analytically obtained bifurcation set in the  $(\chi-d_0)$  space is shown in Fig. 2. The details of the analytical method, available in Refs. [10] and [11], are omitted here. One obtains several windows of periodic solutions having a period of approximately 6.6. Only two such windows are shown in

Fig. 2. The number of collisions per cycle for window 1 is different from that for window 2. The parameter regimes separating the periodic windows correspond to various complicated dynamics including chaos. The right stability boundary of each such window is shown to correspond to a saddle-node instability. For a constant value of  $\chi$ , if  $d_0$  is increased across these saddle-node boundaries, type I intermittency occurs as also confirmed by numerical simulations. One such intermittent signature is shown in Fig. 3. The average laminar length  $\langle \ell \rangle$  of this type of intermittency is found to comply with the law

$$\langle \ell \rangle \sim \mu^{-\delta} \text{ with } \delta \sim 0.520 \pm 0.001,$$

where  $\mu = d_0 - d_0^c$  and  $d_0^c$  is the bifurcation threshold. For further details see Ref. [11].

**B. Type II intermittency**

From this section onwards only the forced system will be considered by assigning a nonzero value of  $F_0$ . It was found that in a significantly wide parameter zone, stable symmetric solutions having two collisions per cycle occur. The zone of the stable solutions with symmetric two impacts per cycle is delineated in the  $(r_m - d_0)$  plane as shown in Fig. 4. The local stability analysis reveals that both the stability boundaries (marked as  $AB$  and  $CD$ ) correspond to Hopf bifurcation. As the nonlinear stability analysis is too complicated, the nature of the bifurcation is not established analytically. However, it is well known that two possibilities exist when a periodic motion encounters a Hopf bifurcation (secondary Hopf bifurcation or Neimark bifurcation). Either a quasiperiodic motion results (when the bifurcation is supercritical) or a more complicated evolution (when the bifurcation is subcritical) having a local-global or entirely global feature ap-

pears. In the present case, the boundary  $AB$  turns out to be a supercritical bifurcation line since the subsequent motion was found to be strictly quasiperiodic. However, when a parameter is varied (here  $d_0$  is decreased while keeping  $r_m$  constant) across the boundary  $CD$ , an intermittent evolution appears. Such an intermittent signature is shown in Fig. 5. A closer look into the signature reveals two distinct phases of the motion. One of these consists of a frequency modulated oscillation (so called laminar phase) with diverging envelopes. Two such phases are punctuated by other phases which are apparently disordered (chaotic phase). According to the classical Pomeau-Manneville [1-3] categorization of different types of intermittencies based on local bifurcations, the present intermittency is of a type II since the preceding bifurcation is a Hopf bifurcation. This indirectly implies that the Hopf bifurcation on the boundary  $CD$  is subcritical. It can be seen from Fig. 6 that the average length  $\langle \ell \rangle$  of the laminar phases complies with the following scaling law predicted by Pomeau-Manneville:

$$\langle \ell \rangle \sim \ln(1/\mu),$$

where  $\mu = d_0 - d_0^c$  and  $d_0^c$  is the bifurcation threshold. Here, it is worth mentioning that though the type II intermittency is known to exist, it rarely occurs in physical systems. Only very few examples are found in the literature [4,5].

**C. Type III intermittency**

The boundaries corresponding to a supercritical Hopf bifurcation are delineated in Figs. 4, 7, and 8. When a parameter is varied (keeping the other constant) across these boundaries, the symmetric, two impacts per cycle solution bifurcates to a quasiperiodic solution. Such quasiperiodic motions can lead to chaos with further variation of the con-

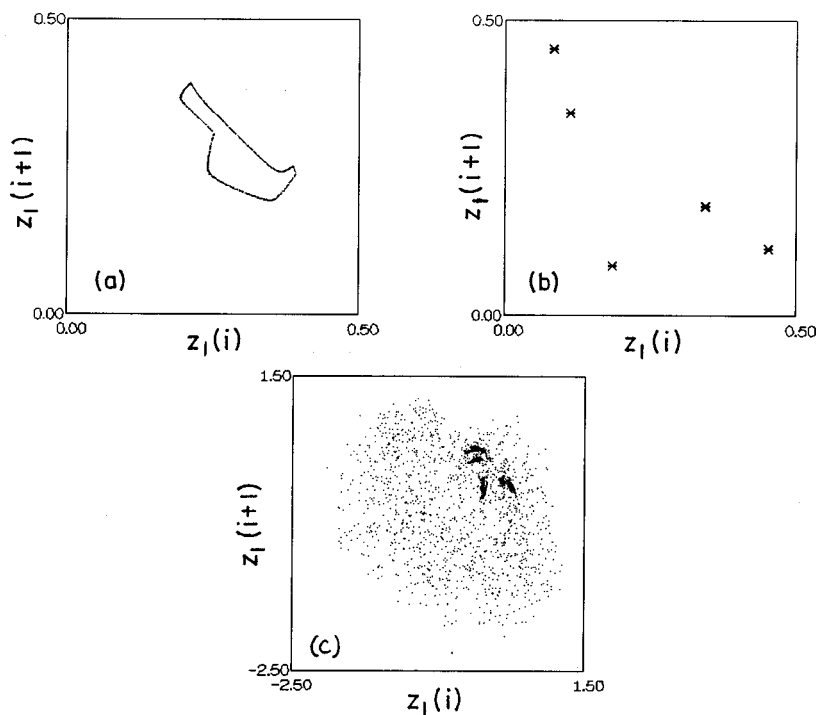


FIG. 9. Quasiperiodic route to chaos via frequency locking.  $F_0=0.5$ ,  $d_0=1.67$ ,  $r_m=0.45$ ,  $\varepsilon=0.1$ ,  $\chi=0.7$ . (a)  $\Omega=1.12$ , (b)  $\Omega=1.125$ , (c)  $\Omega=1.138$ .

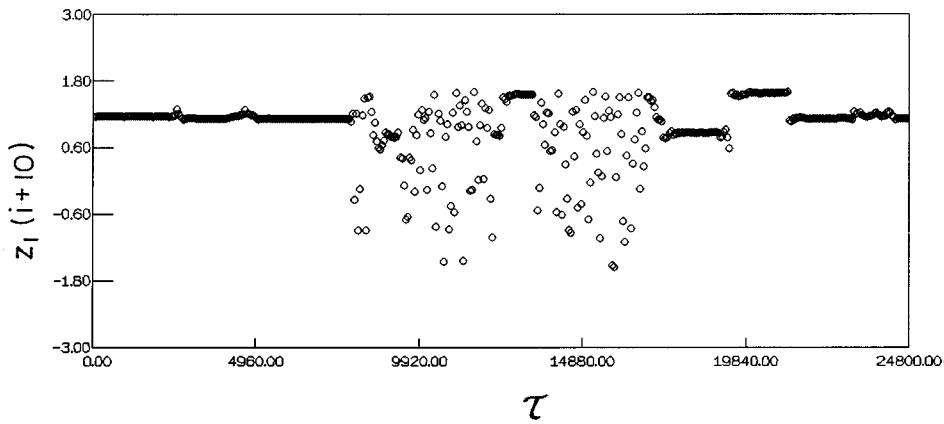


FIG. 10. Type III intermittency. The parameter values are given in Fig. 9(c).

control parameter beyond the bifurcation line. Several routes to chaos via quasiperiodicity have been reported in the literature [3,6,7,11,12]. One of these routes shown in Fig. 9 is via frequency locking. The period of the locked motion in Fig. 9(b) is five times that of the forcing. The locked motion may be destabilized in a number of ways leading to chaos. However, in the present study, the locked modes are seen to undergo intermittent transition to chaos. One such intermittent motion is shown in Fig. 10 in terms of the time history of Poincaré iterates. It is seen from Fig. 9(b) that the motion just before the onset of intermittency is of period 5 and the laminar phase of Fig. 10 corresponds to period 10 [since  $Z(i+10)$  remains constant]. Therefore this intermittency is identified to have arisen out of a subcritical half subharmonic instability, i.e., subcritical period doubling. Thus according to PM classification this is a type III intermittency. The entire sequence may be summarized as follows:

periodic → quasiperiodic → locked mode  
 → intermittency → chaos.

Apart from the above quasiperiodic route to chaos via intermittency, other types of quasiperiodic routes are also detected in this model. One of the routes (Fig. 11) depicts the continuous dispersal of the Poincaré iterates as the control parameter is increased. This route complies with that of the Rayleigh-Benard convection: structure *C* described in Ref. [3].

**D. Intermittency after subcritical pitchfork bifurcation**

The zones of the stable two impacts per cycle solution are delineated in Fig. 8 in the  $F_0$  vs  $\Omega$  plane. It can be analytically shown that the boundary *AB* in this figure corresponds to a subcritical pitchfork bifurcation. Immediately after this bifurcation ( $\Omega$  is decreased across the boundary while keeping  $F_0$  constant), the intermittent motion shown in Fig. 12 appears. In this figure, the time history of the Poincaré iterates (the so-called strobe map with the strobe frequency  $\Omega$ ) is plotted. This kind of intermittency produced by a subcritical pitchfork bifurcation has not been reported so far.

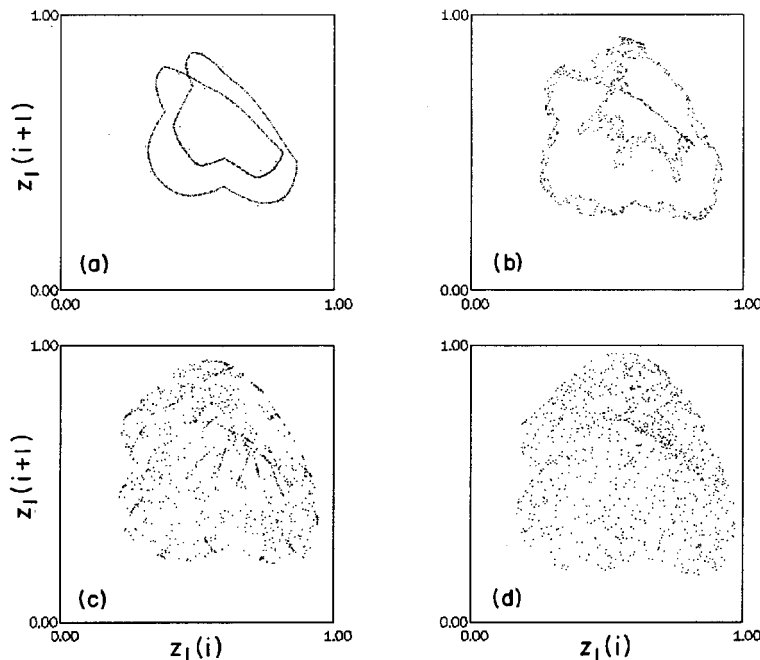


FIG. 11. Quasiperiodic route to chaos.  $F_0=0.5$ ,  $\Omega=1$ ,  $r_m=0.25$ ,  $\chi=0.6$ ,  $\varepsilon=0.1$ . (a)  $d_0=3.35$ , (b)  $d_0=3.37$ , (c)  $d_0=3.38$ , (d)  $d_0=3.39$ .

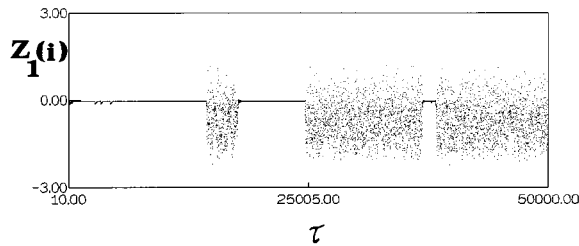


FIG. 12. Intermittency after subcritical pitchfork (symmetry-breaking) bifurcation.  $F_0=0.5$ ,  $d_0=1.6$ ,  $r_m=0.45$ ,  $\varepsilon=0.1$ ,  $\chi=0.7$ ,  $\Omega=0.9512$ .

Theoretical models of the dynamics of intermittency have been put forward by Pomeau-Manneville [1–3]. For describing the mechanism of intermittency they used nonlinear maps which may stand for the suitable Poincaré maps of the periodic solutions of an ordinary differential equation. In their model, a kind of narrow channeling effect accounts for the laminar phase and a proper reinjection principle explains the recontinuation of the laminar phase after a chaotic burst. As the whole mechanism is based on the availability of a suitable nonlinear map, only three types of intermittency could be explained, each corresponding to a type of local

bifurcation viz., saddle-node (type I), subcritical Hopf bifurcation (type II), and subcritical period doubling bifurcation (type III), of the fixed points of the map. However, the pitchfork bifurcation (or symmetry breaking) of a periodic solution of a differential equation does not have any counterpart in the bifurcation of a fixed point of a nonlinear map. Perhaps this is why no model has been studied for the prediction of the intermittency following a pitchfork bifurcation. Another reason may be that the symmetry breaking is a nongeneric bifurcation in the sense that, it is structurally unstable under asymmetric perturbations however small. Of course, for a more detailed study of the mechanism of this type of intermittency, a model should be based on a low dimensional differential equation rather than a nonlinear map.

#### IV. CONCLUSIONS

Three different types of classical, PM intermittencies are detected in a single mechanical model. The possibility of the existence of a new kind of intermittency via a subcritical pitchfork bifurcation (symmetry breaking) is demonstrated through the present model. It is well known that a great deal of hydrodynamic instabilities are related to different kinds of intermittency catastrophes and quasiperiodic transitions. The present model, a purely mechanical one, demonstrates a variety of similar instabilities.

- 
- [1] Y. Pomeau and P. Manneville, *Commun. Math. Phys.* **74**, 189 (1980).
  - [2] P. Manneville and Y. Pomeau, *Physica D* **1**, 219 (1980).
  - [3] P. Berge, Y. Pomeau, and C. Vidal, *Order Within Chaos, Towards a Deterministic Approach to Turbulence* (Wiley, New York, 1984).
  - [4] E. Ringuet, C. Roze, and G. Gouesbet, *Phys. Rev. E* **47**, 1405 (1993).
  - [5] B. Blazejczyk, T. Kapitaniak, and J. Wojewoda, *J. Sound Vib.* **178**, 272 (1994).
  - [6] R. Ecke and H. Haucke, *J. Stat. Phys.* **54**, 1153 (1989).
  - [7] J. P. Gollub and S. V. Benson, *J. Fluid Mech.* **100**, 449 (1980).
  - [8] S. Chatterjee, A. K. Mallik, and A. Ghosh, *J. Sound Vib.* (to be published).
  - [9] S. Chatterjee, A. K. Mallik, and A. Ghosh, *J. Sound Vib.* **187**, 403 (1995).
  - [10] S. Chatterjee, A. K. Mallik, and A. Ghosh, *J. Sound Vib.* (to be published).
  - [11] S. Chatterjee and A. K. Mallik, *J. Sound Vib.* (to be published).
  - [12] D. A. Rand, S. Ostlund, J. Sethna, and E. Siggia, *Phys. Rev. Lett.* **49**, 132 (1982); *Physica D* **8**, 303 (1983).